Spin effects in neutrino scattering by astrophysical black holes

Mridupawan Deka (JINR)

and

Maxim Dvornikov (IZMIRAN and JINR)

Сессия-конференция Секции ядерной физики ОФН РАН «Физика фундаментальных взаимодействий»
ИЯФ СО РАН (г.Новосибирск)

13th March, 2026

References

M. Deka and M. Dvornikov, Review Article
Mod. Phys. Lett. A, Vol. 40, No. 36 (2025) 2530013.

M. Deka and M. Dvornikov
Phys.Atom.Nucl. 88 (2025) 3, 513-519.

M. Deka and M. Dvornikov
Phys.Atom.Nucl. 87 (2024) 4, 483-488.

M. Dvornikov
JCAP 09 (2023) 039.

M. Deka and M. Dvornikov
arXiv:2510.26621.

M. Deka and M. Dvornikov
arXiv:2504.07816.

Neutrino Magnetic Moment

- In minimally extended Standard Model, neutrinos acquire electromagnetic properties through quantum loops effects.
  See talks by A. I. Studenikin and A. R. Popov.
  Detailed review: C. Giunti, A. I. Studenikin, 2014; C. Giunti et. al, 2024.
- Finite neutrino masses and mixing leads to neutrinos having nonzero magnetic moments.
- Upper bounds from experimental and astrophysical measurements, e.g.

$$\begin{aligned} \text{GEMMA} &: \mu_{\nu_e} < 2.9 \times 10^{-11}\mu_{\rm B} \\ \text{CONUS} &: \mu_{\nu_e} < 7.5 \times 10^{-11}\mu_{\rm B} \\ \text{Dresden-II} &: \mu_{\nu_e} < 2.1 \times 10^{-10}\mu_{\rm B} \\ \text{Super-Kamiokande} &: \mu_{\rm S}^{\rm HE} < 1.1 \times 10^{-10}\mu_{\rm B} \\ \text{Borexino} &: \mu_{\nu_e} < 3.9 \times 10^{-11}\mu_{\rm B} \\ \text{XMASS-I} &: \mu_{\rm S}^{\rm LE} < 1.8 \times 10^{-10}\mu_{\rm B} \end{aligned}$$

Neutrino Magnetic Moment

- Non-zero μ leads to helicity flipping interaction with the electromagnetic fields.
- Change of neutrino spin direction w.r.t. its momentum within the same flavor $\Rightarrow$ Neutrino Spin Oscillations. Fujikawa and Shrock, 1980.
- $\mu_{ii}^{\mathrm{D}} \simeq 3.2 \times 10^{-19} \left(\frac{m_i}{eV}\right) \mu_{\mathrm{B}}, \quad \mu_{ii}^{\mathrm{M}} = 0.$ R. E. Shrock, 1982.
- Hence, we can consider Dirac neutrinos only.
- We deal only with the ultra-relativistic neutrinos ($m \ll E$). So we assume all the diagonal magnetic moments to be equal.
- For computational purpose, we choose μ to be closer to the experimental upper bound.

Testing Ground

- Accretion disks in SMBH in some galaxies can be sources of both photons and high energy neutrinos. Chen & Beloborodov, 2006.

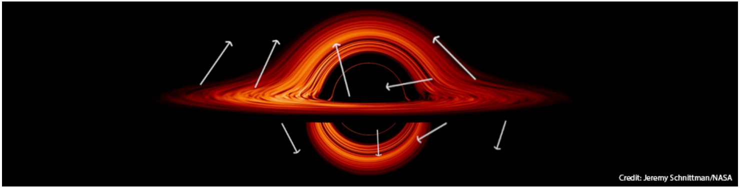

Credit: NASA's Goddard Space Flight Center/Jeremy Schnittman (Image modified by M. Deka).

- White arrows represent neutrino emissions.

Testing Ground

- Before arriving at the observer, these neutrinos move in strong gravitational field near BH.
- Their spins can precess in the presence of external fields of the accretion disk, and they become right handed.
- Right-handed neutrinos are considered to be sterile.
- We shall observe an effective reduction of the initial neutrino flux.

This Work

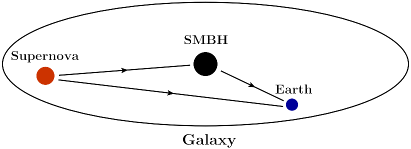

- However, it is computationally complex and expensive to directly deal with the realistic situation.
- Instead, we consider a uniform flux of ultra-relativistic left-polarized Dirac neutrinos coming from a far object, such as a distant core-collapsing supernova.
- They approach a BH at an angle, θ_i, w.r.t. to the BH spin, so that $(r, \theta, \phi)_{\text{source}} = (\infty, \theta_i, 0)$.
- They are either captured or scattered by the BH.

This Work

- We are interested only in the scattered neutrinos.
- We consider a thick accretion disk surrounding the BH with only the toroidal magnetic field.
- The scattered Neutrinos undergo interactions with the matter and magnetic fields in the disk resulting spin precession.
- Some of the left handed neutrinos can become right handed.
- We finally look at the probability distributions of the handedness of the neutrinos at the observer position $(\theta, \phi)_{\mathrm{obs}}$.

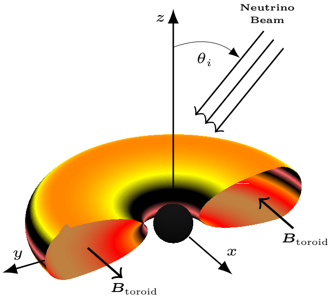
Neutrino
Beam
z
θ_i
y
x
B_{toroid}
B_{toroid}

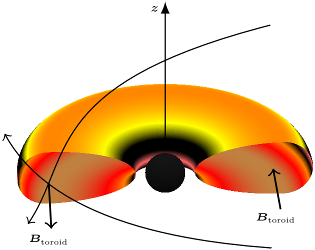
z
B_{toroid}
B_{toroid}

Kerr Metric

- We describe the spacetime of a spinning black hole in Kerr metric.
- Boyer-Lindquist coordinates, $x = (t, r, \theta, \phi)$:

$$\begin{aligned} ds^2 &= g_{\mu\nu} dx^\mu dx^\nu = \left(1 - \frac{r r_g}{\Sigma}\right) dt^2 + 2\frac{r r_g a \sin^2\theta}{\Sigma} dt d\phi - \frac{\Sigma}{\Delta} dr^2 \\ &- \Sigma d\theta^2 - \frac{\Xi}{\Sigma}\sin^2\theta d\phi^2 \end{aligned} \quad (1)$$

$$\begin{aligned} \Delta &= r^2 - r r_g + a^2, \quad \Sigma = r^2 + a^2\cos^2\theta, \\ \Xi &= (r^2 + a^2)\Sigma + r r_g a^2 \sin^2\theta \end{aligned} \quad (2)$$

- BH mass: $M = r_g/2$.
- BH spin: $J = Ma (0 < a < M)$.

Particle Trajectory

- The radial and polar potentials are given by

$$R = \left[(r^2 + a^2)E - aL\right]^2 - \Delta\left[Q + (L - aE)^2\right] \tag{3}$$

$$\Theta = Q + \cos^2\theta\left(a^2E^2 - \frac{L^2}{\sin^2\theta}\right) \tag{4}$$

E : Particle energy, L : Angular momentum, Q : Carter constant.

- The trajectory of an ultra-relativistic neutrino:

$$\int \frac{dr}{\pm\sqrt{R}} = \int \frac{d\theta}{\pm\sqrt{\Theta}} \tag{5}$$

$$\phi = a\int \frac{dr}{\Delta\sqrt{R}}\left[(r^2 + a^2)E - aL\right] + \int \frac{d\theta}{\sqrt{\Theta}}\left[\frac{L}{\sin^2\theta} - aE\right] \tag{6}$$

- Dimensionless variables:

$$r = xr_g,\ L = yr_gE,\ Q = wr_g^2E^2,\ a = zr_g,\ \tilde{\mathfrak{t}} = \cos\theta \tag{7}$$

- Discrete grid in radial direction.
- For an incoming neutrino

$$I_x = z\sqrt{\tilde{\mathfrak{t}}_+^2 + \tilde{\mathfrak{t}}_-^2}\int_x^\infty \frac{\mathrm{d}x'}{\sqrt{R(x')}} \tag{8}$$

$$\tilde{\mathfrak{t}}_\pm^2 = \frac{1}{2z^2}\left[\sqrt{(z^2-y^2-w)^2+4z^2w} \pm (z^2-y^2-w)\right] \tag{9}$$

- Similar definition for an outgoing neutrino.
- x_{tp} is the turn point: the maximal real root of the equation $R(x) = 0 \Rightarrow$ Minimum value of x.

- Neutrinos approaching the BH from infinity go through $(N-1)$ oscillations between $\pm\tilde{\mathfrak{t}}_+$ before reaching $\tilde{\mathfrak{t}}$ at the turn point.

$$\tilde{\mathfrak{t}} \in [\tilde{\mathfrak{t}}_i, \pm\tilde{\mathfrak{t}}_+] \cup \underbrace{[+\tilde{\mathfrak{t}}_+, -\tilde{\mathfrak{t}}_+] \cup \cdots \cup [-\tilde{\mathfrak{t}}_+, +\tilde{\mathfrak{t}}_+]}_{(N-1)\text{ times}} \cup [+\tilde{\mathfrak{t}}_+, \tilde{\mathfrak{t}}]. \tag{10}$$

  - Upper neutrinos: $\tilde{\mathfrak{t}}$ is increasing to $+\tilde{\mathfrak{t}}_+$ in the first segment.
  - Lower neutrinos: $\tilde{\mathfrak{t}}$ is decreasing to $-\tilde{\mathfrak{t}}_+$ in the first segment.
- For an incoming upper neutrino

$$\tilde{\mathfrak{t}}(x) = \cos\theta(x) = \tilde{\mathfrak{t}}_+ \mathrm{cn}\left((-1)^N \left\{F - I_x + 4K\left\lfloor \frac{N}{2} \right\rfloor\right\} \middle| \frac{\tilde{\mathfrak{t}}_+^2}{\tilde{\mathfrak{t}}_-^2 + \tilde{\mathfrak{t}}_+^2}\right) \tag{11}$$

$$N = \left\lfloor \frac{I_x - F}{2K} \right\rfloor + 1, F \equiv F\left(\arccos\frac{\tilde{\mathfrak{t}}_i}{\tilde{\mathfrak{t}}_+}, \frac{\tilde{\mathfrak{t}}_+^2}{\tilde{\mathfrak{t}}_+^2 + \tilde{\mathfrak{t}}_-^2}\right), K \equiv \left(\frac{\tilde{\mathfrak{t}}_+^2}{\tilde{\mathfrak{t}}_+^2 + \tilde{\mathfrak{t}}_-^2}\right) \tag{12}$$

- Similarly for incoming lower neutrinos, and outgoing upper and lower neutrinos.
- Computation of ϕ involves (In)complete elliptic integrals of third kind.

Black Hole Shadow Curve

- We are interested in scattered neutrinos only.
- The edge between the scattered and captured neutrinos is given by $R(\tilde{x}) = R'(\tilde{x}) = 0 \Rightarrow$ BH Shadow curve.
- Additional condition for $\tilde{\mathfrak{t}}_i \neq 0$

$$\tilde{\mathfrak{t}}_i \leq \tilde{\mathfrak{t}}_+ \Rightarrow w \geq -z^2\tilde{\mathfrak{t}}_i^2 + y^2\frac{\tilde{\mathfrak{t}}_i^2}{1-\tilde{\mathfrak{t}}_i^2} \tag{13}$$

- All neutrinos inside the grey area are discarded from the computation.

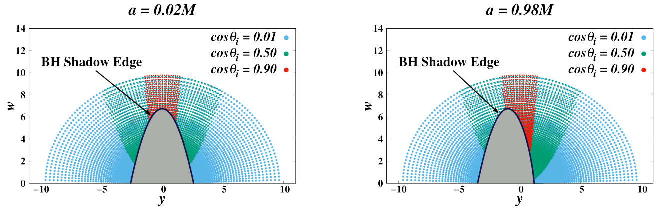

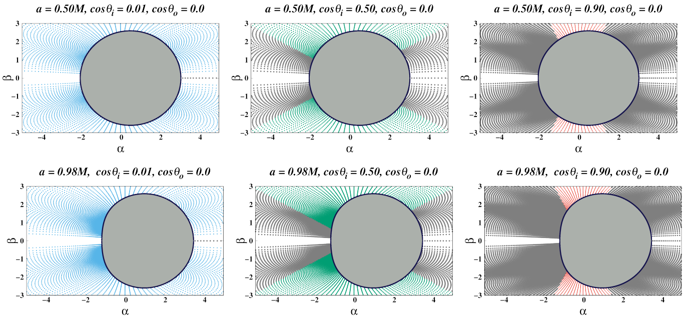

Trajectories of Scattered Neutrinos

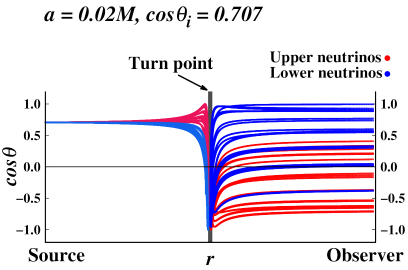

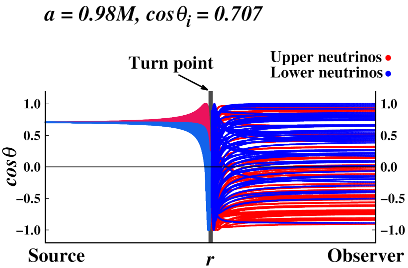

Spin evolution in curved Space-time

- The covariant equation for the neutrino spin four-vector (Dvornikov, 2013; Pomeransky and Khriplovich, 1998),

$$\frac{DS^\mu}{D\tau} = 2\,\mu\left(F^{\mu\nu}S_\nu - U^\mu U_\nu F^{\nu\lambda}S_\lambda\right) + \sqrt{2}G_F\frac{\epsilon^{\mu\nu\lambda\rho}}{\sqrt{-g}}G_\nu U_\lambda S_\rho, \quad \frac{DU^\mu}{D\tau} = 0. \tag{14}$$

- We make a transformation to a local Minkowskian frame.

$$x_a = e_a^\mu x_\mu, \quad \eta_{ab} = e_a^\mu e_b^\nu g_{\mu\nu}, \quad \eta_{ab} = (1, -1, -1, -1) \tag{15}$$

- After making a boost to the particle rest frame, the neutrino invariant 3-spin vector can then be defined as

$$\frac{d\boldsymbol{\zeta}}{dt} = 2(\boldsymbol{\zeta} \times \boldsymbol{\Omega}), \quad \boldsymbol{\Omega} = \boldsymbol{\Omega}_{\mathrm{g}} + \boldsymbol{\Omega}_{\mathrm{em}} + \boldsymbol{\Omega}_{\mathrm{matter}}. \tag{16}$$

  Dvornikov, 2023.

- $\boldsymbol{\Omega}$ can be explicitly calculated in a given metric.

Effective Schrödinger Equation

- Instead, we solve the effective Schrödinger equation for the neutrino polarization,

$$i\,\frac{d\psi}{dx} = H_x\,\psi \tag{17}$$

$$\hat{H}_x = -\mathcal{U}_2(\boldsymbol{\sigma}\cdot\boldsymbol{\Omega}_x)\mathcal{U}_2^{\dagger}, \quad \boldsymbol{\Omega}_x = r_g\boldsymbol{\Omega}\frac{\mathrm{d}t}{\mathrm{d}r}, \quad \mathcal{U}_2 = \exp(\mathrm{i}\pi\sigma_2/4) \tag{18}$$

- We use four-step Adams-Bashforth and Adams-Moulton predictor-corrector method to solve for ψ.
- For an incoming left polarized neutrino, $\psi^T_{-\infty} = (1, 0)$.
- For an outgoing neutrino, it becomes, $\psi^T_{+\infty} = (\psi^{(R)}_{+\infty}, \psi^{(L)}_{+\infty})$.
- The probability of a neutrino remaining left polarized: $P_{\mathrm{LL}} = |\psi^{(L)}_{+\infty}|^2$.

$$\Omega = \Omega_g + \Omega_{matter} + \Omega_{em}$$

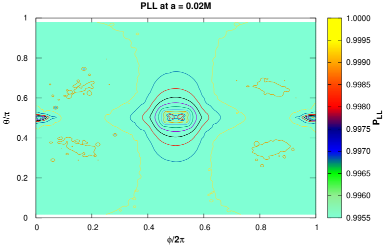

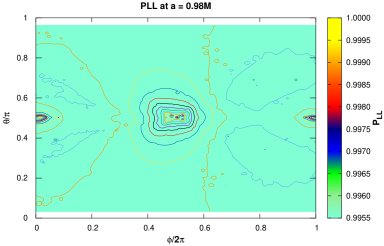

Magnetic fields in the Accretion Disk

- Thick accretion disk surrounding the BH (Polish doughnut). Abramowicz et al., 1978.
- Only toroidal magnetic field inside the disk (Komissarov, 2006)

$$B^{\phi} = \sqrt{\frac{2p_m^{(\text{tor})}}{|g_{\phi\phi} + 2l_0 g_{t\phi} + l_0^2 g_{tt}|}}, \quad B^t = l_0 B^{\phi} \tag{19}$$

$$p_m^{(\text{tor})} = K_m \mathcal{L}^{\kappa-1} \left[\frac{\kappa - 1}{\kappa} \frac{W_{\text{in}} - W}{K + K_m \mathcal{L}^{\kappa-1}} \right]^{\frac{\kappa}{\kappa-1}}, \mathcal{L} = g_{tt} g_{\phi\phi} - g_{t\phi}^2 \tag{20}$$

- The form of the disk depends on the potential,

$$W(r, \theta) = \frac{1}{2} \ln \left| \frac{g_{tt} g_{\phi\phi} - g_{t\phi}^2}{g_{\phi\phi} + 2l_0 g_{t\phi} + l_0^2 g_{tt}} \right| \tag{21}$$

- We consider both co-rotating and counter-rotating disks.

Numerical Parameters

- The mass of SMBH is $10^8 M_\odot$. The BH spin is $0 < a < 0.98M$.
- The maximal strength of the toroidal fields is 320 G. It is 1% of the Eddington limit for this BH mass Beskin, 2010.
- The maximal matter density of hydrogen plasma is 10^{18} cm^{-3}. Such density can be found in some AGN Jiang et al., 2019.
- We consider Neutrino magnetic moment, $\mu = 10^{-13}\mu_\mathrm{B}$. It is below the best astrophysical constraint Viaux et al., 2013.
- The number of scattered neutrinos for each combination of a and θ_i is more than 2 million.
- All the computations have been carried out at Govorun Supercluster of JINR. We have used more than 2000 SkyLake and IceLake processors continuously for several weeks.

Co-rotating Disk

$$\mathbf{\Omega} = \mathbf{\Omega}_{\rm g} + \mathbf{\Omega}_{\rm matter} + \mathbf{\Omega}_{\rm em}$$

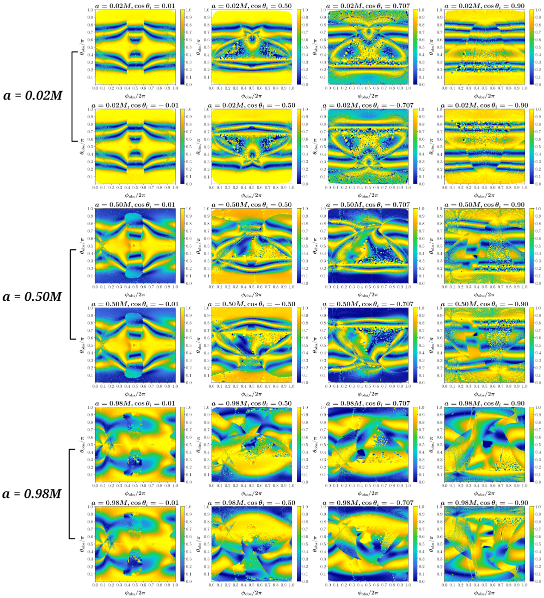

Counter-rotating Disk

$$\boldsymbol{\Omega} = \boldsymbol{\Omega}_{\mathrm{g}} + \boldsymbol{\Omega}_{\mathrm{matter}} + \boldsymbol{\Omega}_{\mathrm{em}}$$

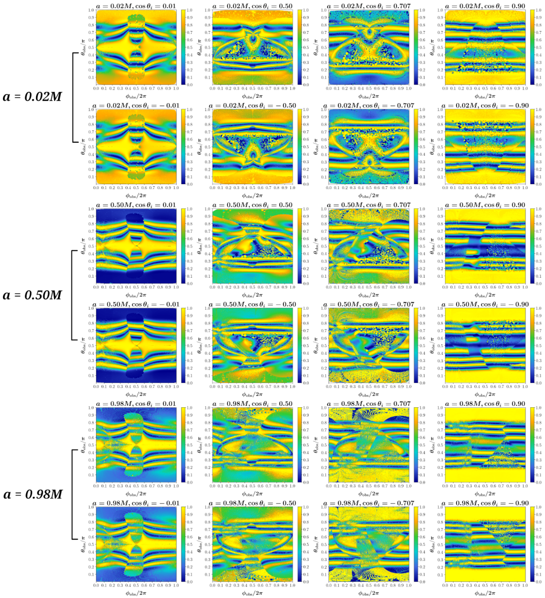

Conclusion

- Only toroidal magnetic field is sufficient enough for spin oscillations to occur.

- We investigate P_{LL} for a number of different θ_i's. This is important since the relative position between a neutrino source and Earth is not known during the observation.

Conclusion

- There is a clear difference between $P_{\rm LL}$'s for the co-rotating and counter-rotating disks even for a slowly rotating BH.

Co-rotating Disk

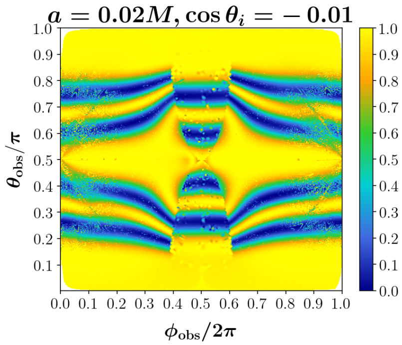

Counter-rotating Disk

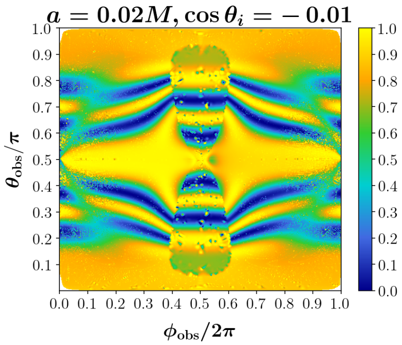

Conclusion

- No symmetric distributions of P_{LL} w.r.t. the $\theta_{\mathrm{obs}} = \pi/2$ plane can be seen for a rotating BH at lower $\cos\theta_i$'s.

Co-rotating Disk

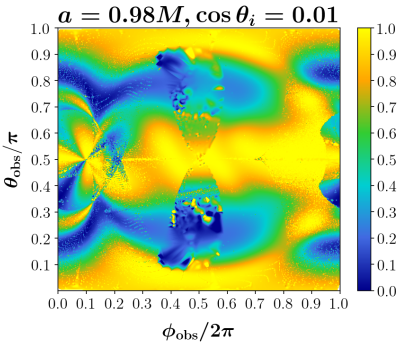

Counter-rotating Disk

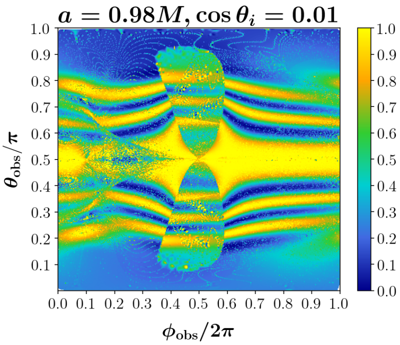

Conclusion

- No inverse symmetry of P_{LL} for the opposite values of $\cos\theta_i$ with the same BH spin is exhibited for a rotating BH.

Co-rotaing Disk

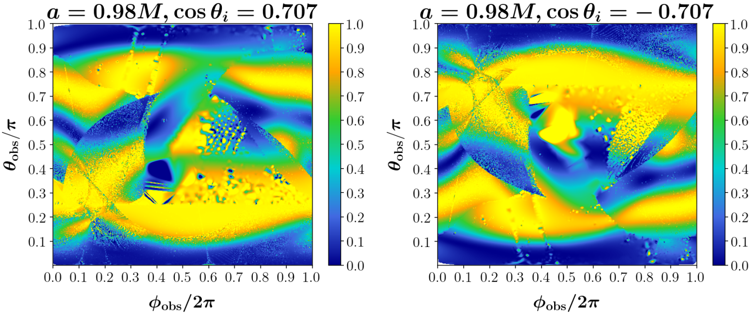

Thank you!

Extras